Differential Contribution of Active Site Residues in Substrate Recognition Sites 1 and 5 to Cytochrome P450 2C8 Substrate Selectivity and Regioselectivity†

Oranun Kerdpin,‡,§ David J. Elliot,‡ Sanford L. Boye,‡ Donald J. Birkett,‡ Krongtong Yoovathaworn,§ and John O. Miners*,‡

Department of Clinical Pharmacology, Flinders University and Flinders Medical Centre, Adelaide, SA 5042, Australia, and Department of Pharmacology, Faculty of Science, Mahidol University, Bangkok 10400, Thailand

Received February 11, 2004; Revised Manuscript Received April 22, 2004

ABSTRACT: Selected active site residues in substrate recognition sites (SRS) 1 and 5 of cytochrome P450 2C8 (CYP2C8) were mutated to the corresponding amino acids present in CYP2C9 to investigate the contribution of these positions to the unique substrate selectivity and regioselectivity of CYP2C8. The effects of mutations, singly and in combination, were assessed from changes in the kinetics of paclitaxel 6α-hydroxylation, a CYP2C8-specific pathway, and the tolylmethyl and ring hydroxylations of torsemide, a mixed CYP2C9/CYP2C8 substrate. Within SRS1, the single mutation S114F abolished paclitaxel 6α-hydroxylation, while the I113V substitution resulted in modest parallel reductions in K_m and V_{max}. Mutations in SRS5 (viz., V362L, G365S, and V366L) reduced paclitaxel intrinsic clearance (V_{max}/K_m) by 88−100%. Torsemide is preferentially metabolized by CYP2C9, and it was anticipated that the mutations in CYP2C8 might increase activity. However, methyl and ring hydroxylation intrinsic clearances were either unchanged or decreased by the mutations, although hydroxylation regioselectivity was often altered relative to wild-type CYP2C8. The mutations significantly increased (28−968%) K_m values for both torsemide methyl and ring hydroxylation but had variable effects on V_{max}. The effects of the combined mutations in SRS1, SRS5, and SRS1 plus SRS5 were generally consistent with the changes produced by the separate mutations. Mutation of CYP2C8 at position 359 (S359I), a site of genetic polymorphism in CYP2C9, resulted in relatively minor changes in paclitaxel- and torsemide-hydroxylase activities. The results are consistent with multiple substrate binding orientations within the CYP2C8 active site and a differential contribution of active site residues to paclitaxel and torsemide binding and turnover.

Cytochromes P450 (CYP)[1] involved in the metabolism of drugs and other xenobiotics characteristically exhibit distinct but not uncommonly overlapping substrate selectivities (*1*, *2*). In addition, differences in substrate regio- and stereoselectivity may occur between CYPs. Given the pharmacological and toxicological significance of these enzymes, the molecular basis of the unique substrate selectivities and regio- and stereoselectivities of human xenobiotic metabolizing CYPs has attracted considerable attention. In particular, site-directed mutagenesis, chimeragenesis, and homology modeling employing the X-ray crystal structures of bacterial CYPs as templates have been widely used to investigate structure−function relationships of mammalian CYPs (*3*). These studies provide support for the proposal of Gotoh (*4*) that six substrate recognition sites (SRS) are generally conserved among most CYPs. Elucidation of the X-ray crystal structure of rabbit CYP2C5 (*5*) allowed the generation of refined homology models of human CYPs, especially CYP2C enzymes (for example *6*, *7*), and the recent availability of a crystal structure for a human enzyme (viz., CYP2C9) (*8*) may result in more predictive models.

The human CYP2C subfamily comprises four members, CYP2C8, CYP2C9, CYP2C18, and CYP2C19. Of these, CYP2C9 ranks among the most important drug-metabolizing enzymes (*9*). For example, CYP2C9 is responsible for the elimination of losartan, phenytoin, *S*-warfarin, and many nonsteroidal antiinflammatory agents and sulfonylurea hypoglycemics. While it was previously believed that CYP2C8 had a limited role in drug metabolism, accumulating evidence indicates that the contribution of CYP2C8 to drug metabolism in humans has been underestimated. CYP2C8 is known to play a major role in the metabolism of amodiaquine (*10*), cerivastatin (*11*), chloroquine (*12*), paclitaxel (*13*), repaglinide (*14*), rosiglitazone (*15*), verapamil (*16*), and zopiclone (*17*). Moreover, there is evidence for a physiological role of CYP2C8 in arachidonic acid (*18*) and retinoic acid (*19*) biotransformation. Despite growing awareness of the importance of CYP2C8 in the metabolism of drugs and endogenous compounds, no studies have directly investigated the contribution of putative active site residues to substrate selectivity and regioselectivity. In contrast, site-directed mutagenesis has been employed widely to assess the effects of numerous SRS and non-SRS residues on CYP2C9 activity and substrate selectivity (*20*−*26*). Moreover, several CYP2C9

† This work was supported by a grant from the National Health and Medical Research Council of Australia.

* Corresponding author. E-mail: john.miners@flinders.edu.au. Telephone: 61-8-82044131. Fax: 61-8-82045114.

‡ Flinders University and Flinders Medical Centre.

§ Mahidol University.

[1] Abbreviations: CYP, cytochrome P450; DES, diethylstilbestrol; HPLC, high-performance liquid chromatography; K_m, Michaelis constant; 4-MU, 4-methylumbelliferone; CPR, NADPH cytochrome P450 reductase; SRS, substrate recognition site; V_{max}, maximal velocity.

10.1021/bi0496844 CCC: $27.50
Published on Web 05/26/2004

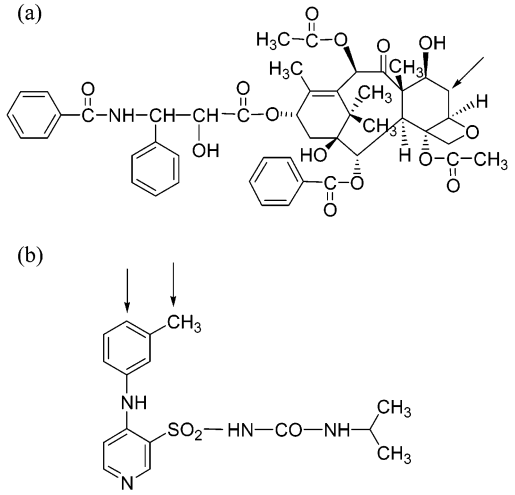

FIGURE 1: Structures of paclitaxel (a) and torsemide (b). The arrows indicate the sites of CYP2C8-catalyzed hydroxylation.

homology models have been generated using CYP2C5 as the template (*6*, *7*, *25*, *27*, *28*), but modeling of CYP2C8 has been more limited (*6*, *28*).

Although CYP2C8 and CYP2C9 share 78% sequence identity (and 85% similarity), they exhibit relatively minor overlap in substrate and inhibitor selectivity. Torsemide and tolbutamide are metabolized by both CYP2C8 and CYP2C9, although intrinsic clearances (V_{max}/K_m) are typically an order of magnitude higher for CYP2C9 (*20*, *29*). Similarly, the prototypic CYP2C9 inhibitors sulfaphenazole and fluconazole have a minor effect on CYP2C8 activity (*29*, *30*). Thus, CYP2C8 and CYP2C9 represent a useful model for investigating the role of SRS residues in the differential substrate selectivity and regioselectivities within the CYP2C subfamily. The recent availability of human CYP2C homology models based on the X-ray crystal structure of CYP2C5 provides a basis for a systematic approach to the characterization of CYP2C8 structure−function relationships. These models generally locate residues 113 and 114 of SRS1 and residues 361−366 of SRS5 within the putative CYP2C8 and CYP2C9 active sites. CYP2C8 and CYP2C9 differ at residues 113 (I → V), 114 (S → F), 362 (V → L), 365 (G → S), and 366 (V → L). Thus, to investigate the contribution of these amino acids to CYP2C8 substrate selectivity and regioselectivity, residues 113, 114, 362, 365, and 366 of CYP2C8 were mutated to the corresponding amino acids present in CYP2C9, initially in combination and then singly. Additionally, residue 359 of CYP2C8 was mutated to the corresponding amino acid of CYP2C9 (i.e., S → I). Although homology models locate residue 359 outside the putative CYP2C8 and CYP2C9 active sites, amino acid substitution at this position is known to reduce CYP2C9 activity. Indeed, polymorphism at this site is responsible for the CYP2C9 poor-metabolizer phenotype (*9*, *31*, *32*).

The effects of mutations were assessed by measurement of paclitaxel 6α-hydroxylation and torsemide tolylmethyl and ring hydroxylation (Figure 1) kinetic parameters. Paclitaxel 6α-hydroxylation is catalyzed solely by CYP2C8 (*13*), while torsemide is a mixed CYP2C9/CYP2C8 substrate (*29*). Whereas the substitutions at positions 114, 362, 365, and 366 abolished or greatly reduced paclitaxel 6α-hydroxylation, they resulted in more subtle changes in torsemide hydroxylation regioselectivity. The results are consistent with multiple substrate binding orientations within the CYP2C8 active site and a differential contribution of active site residues to paclitaxel and torsemide binding, turnover, or both.

EXPERIMENTAL PROCEDURES

Materials

The CYP2C8 and CYP2C9 cDNAs used in this study have been reported previously (*33*). Professor Ronald W. Estabrook (University of Texas Southwestern Medical Center, Dallas, TX) kindly provided the OmpA-rat NADPH-CYP reductase (OmpA-CPR) fusion cDNA. Restriction enzymes were purchased from New England Biolabs (Beverly, MA). Oligonucleotides were synthesized by Sigma Genosys (NSW, Australia). *Escherichia coli* DH5α cells were purchased from Invitrogen (Carlsbad, CA). The rabbit anti-human CYP2C8 IgG was obtained from Research Diagnostics Inc (Flanders, NJ). Paclitaxel, diethylstilbestrol (DES), 4-methylumbelliferone (4-MU), NADP, NADPH, glucose 6-phosphate, glucose 6-phosphate dehydrogenase, and cytochrome *c* were purchased from Sigma-Aldrich Co. (St. Louis, MO). 6α-Hydroxypaclitaxel was obtained from BD Gentest (Woburn, MA). Torsemide, methylhydroxytorsemide, and ring-hydroxylated torsemide were a gift from Boehringer Mannheim International (Mannheim, Germany). All other chemicals were of analytical reagent grade.

Methods

Construction of Plasmids. The 5′-terminus of the CYP2C8 cDNA was modified by replacing the native leader sequence with a modified sequence derived from bovine CYP17A followed by a short CYP2C consensus sequence as described by Boye et al. (*33*). The N-terminal modification was introduced by PCR using primers that incorporated the desired modification and *Nde*I and *Hin*dIII sites at the 5′- and 3′-termini, respectively. The PCR product was digested with *Nde*I and *Hin*dIII and ligated into the pCWOri+ plasmid that was previously digested with the same endonucleases. The 5′-terminus of the CYP2C9 cDNA was modified by replacing the second codon with GCT, deleting codons 3−20, and adjusting codons 21−26 for bacterial codon bias (*33*). Studies in this laboratory have demonstrated that the separate 5′-terminus modifications to the CYP2C8 and CYP2C9 cDNAs result in optimal expression of CYP2C8 and CYP2C9 in *E. coli* (*33*).

To generate an active system, CPR was coexpressed with each CYP using separate cotransformed plasmids (*33*). The plasmid pACYC184 (New England Biolabs, Beverly, MA) was used to express rat CPR. The pACYC184 plasmid has a different origin of replication and selective marker conferring compatibility with cotransformed pCW-based expression plasmids. The cDNA coding for CPR consisted of the OmpA signal sequence fused upstream of the full-length native CPR sequence.

Site-Directed Mutagenesis. Two residues (113, 114) in SRS1 and four residues (359, 362, 365, and 366) in SRS5 were mutated to the corresponding amino acids found in CYP2C9, in combination and singly. Mutagenesis was performed using the QuikChange site-directed mutagenesis kit (Stratagene, La Jolla, CA) to produce the nine different CYP2C8 mutants (Table 1). The primers used for mutagen-

Table 1: Primers Used for Site-Directed Mutagenesis[a]

CYP2C8 mutant	template	forward primer
I113V	wild-type	5′-ACTAAAGGACTTGGAATC**G**TTTCCAGCAATGGAAAGAG-3′
S114F	wild-type	5′-AAAGGACTTGGAATCATTT**T**CAGCAATGGAAAGAGATGG-3′
I113V−S114F	wild-type	5′-ACTAAAGGACTTGGAATC**G**TTT**T**CAGCAATGGAAAGAGATGG-3′
S359I	wild-type	5′-GAGATCCAGAGATACA**T**TGACCTTGTCCCCACC-3′
V362L	wild-type	5′-GATACAGTGACCTT**C**TCCCCACCGGTGTG-3′
G365S	wild-type	5′-GACCTTGTCCCCACC**A**GTGTGCCCCATGCAG-3′
V366L	wild-type	5′-GACCTTGTCCCCACCGGT**C**TGCCCCATGCAGTGACC-3′
S359I−V362L−G365S−V366L[b]	S359I	5′-GATACATTGACCTT**C**TCCCCACCGGTGTG-3′
	S359I−V362L	5′-GACCTTCTCCCCACC**A**GT**C**TGCCCCATGCAGTGACC-3′
I113V−S114F−S359I−V362L−G365S−V366L	S359I−V362L−G365S−V366L	5′-ACTAAAGGACTTGGAATC**G**TTT**T**CAGCAATGGAAAGAGATGG-3′

[a] The changed bases are marked in bold. The reverse primers are exactly complementary to the forward primers. [b] S359I mutant was used as a template to generate S359I−V362L, which was then used as a template to produce S359I−V362L−G365S−V366L.

esis are listed in Table 1. Mutations were confirmed by sequencing (ABI Prism 373 DNA sequencer; Applied Biosystems, Foster City, CA).

Expression in E. coli. Plasmids were transformed into *E. coli* DH5α competent cells. Single isolated colonies were grown by shaking at 37 °C overnight in Luria−Bertani medium containing ampicillin (100 mg/L) and chloramphenicol (50 mg/L). Overnight cultures of each clone were diluted 1:100 in Terrific broth containing 0.2% bactopeptone (w/v), ampicillin (100 mg/L), and chloramphenicol (50 mg/L). Cells were grown at 37 °C in a rotary shaker until the optical density at 600 nm reached 0.7, when δ-aminolevulinic acid and isopropyl-β-D-thiogalactopyroside were added to final concentrations of 0.5 mM and 1 mM, respectively. Cultures were then grown at 30 °C with shaking at 200 rpm for 24 h.

Harvesting of Cultures, Membrane Preparations, and Determination of Expression Levels. Bacterial cells were harvested and membrane fractions were prepared according to Gillam et al. (*34*). Protein and CYP content of bacterial membranes were assessed using spectrophotometric methods (*35*, *36*). CPR content was estimated using a spectrophotometric assay for cytochrome *c* reductase activity (*37*), assuming that 1 nmol of CPR reduces 3000 nmol of cytochrome *c* per minute.

Immunoblotting. Proteins were separated by sodium dodecyl sulfate−polyacrylamide gel electrophoresis on 10% acrylamide gels and transferred onto nitrocellulose membranes (Bio-Rad Laboratories, Hercules, CA). Blots were probed with rabbit anti-human CYP2C8 IgG, followed by horseradish peroxidase-conjugated goat anti-rabbit antibody. The BM chemiluminescence blotting substrate (Roche Diagnostics GmbH, Mannheim, Germany) was used for immunodetection. The intensities of the immunoblots were measured with a Bio-Rad model GS-700 imaging densitometer.

Paclitaxel 6α-Hydroxylation Assay. Incubation mixtures, in a total volume of 200 μL contained expressed CYP (2−10 pmol of CYP), a NADPH-generating system (1 mM NADP, 10 mM glucose 6-phosphate, 2 IU of glucose 6-phosphate dehydrogenase, and 5 mM $MgCl_2$), and paclitaxel (using nine substrate concentrations in the range of 0.25−10 μM for kinetic determinations) in 0.1 M phosphate buffer, pH 7.4. After a 5 min preincubation at 37 °C, reactions were initiated by the addition of the NADPH-generating system. The reactions were carried out for 10 min at 37 °C in shaking water bath. The NADPH-generating system was omitted from the blank and replaced by an equal volume of buffer. Under these conditions, rates of product formation were linear with respect to incubation time and CYP concentration. Reactions were terminated by the addition of ice-cold acetonitrile (0.2 mL) containing 0.1 μg of DES (the assay internal standard). After cooling on ice for 5 min, the mixtures were centrifuged (12 000*g*) for 10 min. The supernatant fraction (100 μL) was injected onto an Agilent 1100 HPLC system (Agilent Technologies, Palo Alto, CA). Chromatography was performed using a Nova-Pak C18 column (3.9 mm × 150 mm inner diameter, 4 μm particle size, Waters Corporation, Milford, MA) with a μBondapak C18 Guard-Pak. Peaks were separated with 0.002% glacial acetic acid in 15% acetonitrile (mobile phase A) and 100% acetonitrile (mobile phase B) as follows: initial conditions of 75%A/25%B changed to 60%A/40%B using a linear gradient over 15 min and then to 25%A/75%B over 0.1 min, which was held for 0.5 min before returning to the starting conditions. The mobile phase flow rate was 1.0 mL/min and peaks were monitored by UV detection at 230 nm. Under these conditions, retention times for 6α-hydroxypaclitaxel, DES, and paclitaxel were 10.6, 12.1, and 14.4 min, respectively. Due to the cost of 6α-hydroxypaclitaxel, this metabolite was quantified using a paclitaxel standard curve. The molar extinction of 6α-hydroxypaclitaxel at 230 nm is essentially identical to that of paclitaxel (*38*). Standard curves were constructed in the paclitaxel concentration range 0.05−0.25 μM, standards being treated in the same manner as incubation samples.

Torsemide Hydroxylation Assay. Torsemide methyl and ring hydroxylation activities were measured using a previously published HPLC method with 4-MU as the internal standard (*39*). Kinetics of metabolite formation by CYP2C8 (and CYP2C8 mutants) were determined using nine to eleven substrate concentrations in the range of 25−800 μM in 1 mL incubations containing 50 pmol of CYP. Incubations were carried out for 30 min at 37 °C in shaking water bath. Similarly, the kinetics of CYP2C9-catalyzed torsemide hydroxylation were determined for eight substrate concentrations in the range of 1−100 μM using 10 pmol of CYP and a reaction time of 15 min. Rates of formation of both metabolites were linear with respect to incubation time and CYP concentration.

Data Analysis. Kinetic data are presented as the mean ± standard deviation (SD) of four separate experiments, unless otherwise stated. The kinetic parameters K_m and V_{max} were determined by fitting to the Michaelis−Menten equation

Table 2: Expression Levels of CYP and CPR from Two Plasmid Coexpression System[a]

CYP	CYP (nmol/L of culture)	CPR (nmol/L of culture)	CYP/CPR ratio
CYP2C8			
wild-type	389 ± 70	334 ± 32	1:0.9
I113V−S114F−S359I−V362L−G365S−V366L	285 ± 49	247 ± 55	1:0.9
I113V−S114F	306 ± 74	276 ± 70	1:0.9
I113V	383 ± 91	339 ± 70	1:0.9
S114F	35 ± 4	270 ± 8	1:7.7
S359I−V362L−G365S−V366L	292 ± 51	212 ± 26	1:0.7
S359I	469 ± 51	469 ± 28	1:1.0
V362L	383 ± 27	390 ± 21	1:1.0
G365S	88 ± 7	314 ± 17	1:3.6
V366L	289 ± 30	292 ± 4	1:1.0
CYP2C9			
wild-type	244 ± 26	268 ± 84	1:1.1

[a] Expression levels are mean ± SD of four experiments for wild-type CYP2C8 and CYP2C8 mutants and three experiments for wild-type CYP2C9.

using the program EnzFitter, version 2.0 (Biosoft, Cambridge, UK). Units of V_{max} are pmol/(min pmol of CYP), and hence this parameter is equivalent to k_{cat}. Intrinsic clearance was calculated as V_{max}/K_m. Differences in kinetic parameters between wild-type CYP2C8 and CYP2C8 mutants were tested by one-way ANOVA followed by post-hoc multiple comparisons tests (Tukey HSD or Games−Howell test). Levene's test for homogeneity of variances was used to determine the method of post-hoc analysis. The Tukey HSD test was used when homogeneity of variances could be assumed, while the Games−Howell test was employed when this assumption was not met. Differences were considered statistically significant at $P < 0.05$. Statistical analyses were performed using SPSS for Windows, version 11.5 (SPSS Inc, Chicago, IL).

RESULTS

Expression of CYP and CPR in E. coli. The expression of wild-type CYP2C8 and all mutants in *E. coli* was evaluated by immunoblotting with anti-CYP2C8 IgG. Similar intensities were observed for the nine mutants with the optical densities ranging from 0.18 to 0.38 (compared to 0.19 for wild-type CYP2C8; data not shown). Mean wild-type CYP2C8 expression, estimated from the carbon monoxide difference spectrum, was 389 nmol/L of culture (Table 2). Except for S114F and G365S, expression of all mutants (285−469 nmol/L) was similar to wild-type CYP2C8. Expression levels of the S114F and G365S mutants were 11- and 4-fold lower, respectively, than that of wild-type CYP2C8, although apoenzyme expression (determined by immunoblotting) was similar. The wild-type and mutant CYP2C8 enzymes were coexpressed in *E. coli* with CPR to generate an active system. Levels of coexpressed CPR ranged from 212 to 469 nmol/L for the wild-type enzymes and all CYP2C8 mutants (Table 2). Thus, the CYP to CPR ratios were approximately 1:1, except for the S114F and G365S mutants (1:7.7 and 1:3.6, respectively). Consistent with these results, Melet et al. (*25*) reported that the F114I and S365G mutations in CYP2C9 resulted in low expression. Recent studies in this laboratory demonstrated that CYP2C9 activity increases with increasing CPR to CYP ratios (up to 5:1) when these enzymes are coexpressed in *E. coli* (*33*). Thus, V_{max} and intrinsic clearance values for torsemide hydroxylation by the S114F and G365G mutants (Table 4) may be overestimated relative to the corresponding kinetic parameters for other mutants and wild-type enzymes.

Paclitaxel 6α-Hydroxylation Activity. Wild-type CYP2C8, but not CYP2C9, catalyzed the 6α-hydroxylation of paclitaxel. Paclitaxel 6α-hydroxylation by CYP2C8 exhibited Michaelis−Menten kinetics (Figure 2) as reported previously (*30*). However, the I113V−S114F, S359I−V362L−G365S−V366L, and I113V−S114F−S359I−V362L−G365S−V366L mutants lacked paclitaxel 6α-hydroxylase activity (Table 3). To assess which of these mutations were responsible for the loss of catalytic activity, the individual mutants at each of the six positions were investigated. The mutations at residues 114 (S114F) and 366 (V366L) abolished paclitaxel 6α-hydroxylation, while those at residues 362 (V362L) and 365 (G365S) reduced intrinsic clearance (V_{max}/K_m) by 16.9- and 8.5-fold, respectively (Table 3). The decreased intrinsic clearances associated with the residue 362 and 365 mutants resulted from dual effects on K_m and V_{max}, which were increased and decreased, respectively, relative to wild-type CYP2C8 (Table 3). In contrast, the intrinsic clearances of the I113V and S359I mutants were similar to those of the wild-type CYP2C8, although both the K_m and V_{max} of the I113V mutant were lower (by approximately 40−50%) than those of the wild-type enzyme (Table 3). All mutants exhibiting paclitaxel 6α-hydroxylase activity followed Michaelis−Menten kinetics (Figure 2).

Torsemide Hydroxylation Activity. The kinetic parameters obtained for torsemide hydroxylation by wild-type CYP2C8 and CYP2C9 and by the CYP2C8 mutants are summarized in Table 4. Wild-type CYP2C8 and CYP2C9 generated both methyl- and ring-hydroxylated torsemide. The kinetics of metabolite formation were adequately described by the Michaelis−Menten equation (Figure 3). Although there was a suggestion of deviation from Michaelis−Menten kinetics for torsemide ring hydroxylation by wild-type CYP2C9 at low substrate concentration (Figure 3), fitting of kinetic data to an allosteric model or the Hill equation (with negative cooperativity) produced inferior "goodness of fit" parameters. Methyl hydroxylation represented the major pathway of torsemide metabolism by both wild-type CYP2C8 and CYP2C9 (Table 4), arising from a higher V_{max} (in the absence of a difference in K_m) for this metabolite. Torsemide was more efficiently hydroxylated by CYP2C9 than by CYP2C8, as evidenced by a 54-fold higher intrinsic clearance for methyl hydroxylation and a 16-fold higher intrinsic clearance for ring hydroxylation. Regioselectivity of hydroxylation differed between CYP2C8 and CYP2C9; respective intrinsic clearance ratios for methyl-to-ring hydroxylation were 3.5 and 11.4.

All of the CYP2C8 mutants exhibited torsemide methyl- and ring-hydroxylase activities (Table 4), and kinetic data for all mutants were well-fitted to the Michaelis−Menten equation (data not shown). Compared to wild-type CYP2C8, the I113V−S114F combined mutation reduced methyl-hydroxylation intrinsic clearance by over 80%, primarily due to a reduction in V_{max} (Table 4 and Figure 4). Data for the separate mutations indicated a greater effect of the I113V substitution, although both the individual SRS1 mutations decreased V_{max} and increased K_m for this pathway. As noted

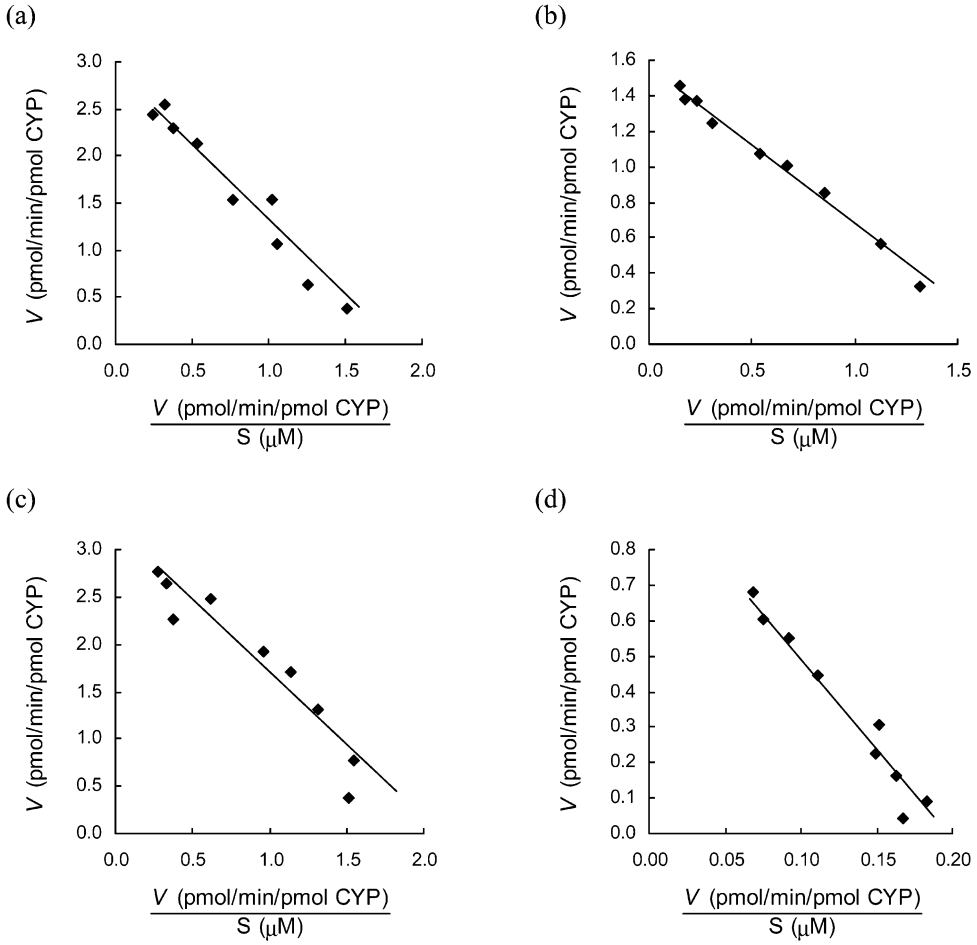

FIGURE 2: Representative Eadie−Hofstee plots for paclitaxel 6α-hydroxylation by CYP2C8: (a) wild-type; (b) I113V; (c) S359I; (d) G365S. Points are experimentally determined values (means of duplicate measurements at each concentration), while the solid lines are the computer-generated curves of best fit.

Table 3: Kinetic Parameters for Paclitaxel 6α-Hydroxylation by Wild-Type CYP2C8 and CYP2C8 Mutants[a]

	paclitaxel 6α-hydroxylation		
CYP2C8	V_{max} (pmol/(min·pmol of CYP))	apparent K_m (μM)	V_{max}/K_m (μL/(min·pmol of CYP))
wild-type	2.67 ± 0.41	1.58 ± 0.18	1.69 ± 0.12
I113V−S114F−S359I−V362L−G365S−V366L	*b*	*b*	*b*
I113V−S114F	*b*	*b*	*b*
I113V	1.53 ± 0.10[c]	0.83 ± 0.09[c]	1.87 ± 0.23
S114F	*b*	*b*	*b*
S359I−V362L−G365S−V366L	*b*	*b*	*b*
S359I	3.28 ± 0.29	1.54 ± 0.20	2.14 ± 0.12[c]
V362L	0.38 ± 0.05[c]	3.77 ± 0.80[c]	0.10 ± 0.01[c]
G365S	0.98 ± 0.07[c]	4.83 ± 0.28[c]	0.20 ± 0.01[c]
V366L	*b*	*b*	*b*

[a] Apparent K_m and V_{max} values are given as mean ± SD of four experiments for wild-type CYP2C8 and CYP2C8 mutants. [b] Not detected. [c] $P < 0.05$ compared to wild-type CYP2C8.

previously, however, the higher CPR to CYP ratio associated with the 114F mutant may overestimate V_{max} (and intrinsic clearance) compared to the mutation at residue 113. In contrast, the I113−S114F combined mutation increased the intrinsic clearance for ring hydroxylation, solely due to increased V_{max} (Table 4, Figure 4). Similarly, each of the I113V and S114F mutations increased V_{max} for this pathway, but both again also increased K_m. The combined S359I−V362L−G365S−V366L mutations had no effect on methyl-hydroxylation intrinsic clearance, although there were small parallel increases (ca. 30%) in both V_{max} and K_m compared to wild-type CYP2C8 (Table 4, Figure 4). Methyl-hydroxylation K_m and V_{max} values also tended to increase in parallel for the mutations at residues 362 and 366, resulting in no significant change in intrinsic clearance. However, intrinsic clearance was reduced by the S359I (−34%) and G365S (−47%) mutations due to decreased V_{max} and increased K_m, respectively. Ring-hydroxylation intrinsic clearance by the S359I−V362L−G365S−V366L combined mutant was reduced by 75% as a result of increased K_m (Table 4, Figure 4). All single substitutions in SRS5 increased K_m for the ring-hydroxylation pathway by 1.4−9.7-fold (Table 4). With the exception of the G365S mutation, all other single substitutions also increased the V_{max} for torsemide ring hydroxylation (1.6−3.2-fold; Table 4). It should be noted that the higher CPR to CYP ratio associated with the 365S mutant may obscure a significant decrease in V_{max} (and hence a larger effect on intrinsic clearance) for both the methyl- and ring-hydroxylation pathways. The largest decreases in intrinsic clearance were observed for methyl hydroxylation by the I113V mutant (−82%) and ring hydroxylation by the V362L and G365S mutants (−68%), the latter due to the large increases in K_m.

Table 4: Kinetic Parameters for Torsemide Hydroxylation by Wild-Type CYP2C8, CYP2C8 Mutants, and Wild-Type CYP2C9[a]

CYP	torsemide methyl hydroxylation			torsemide ring hydroxylation		
	V_{max} (pmol/(min·pmol of CYP))	apparent K_m (μM)	V_{max}/K_m (μL/(min·pmol of CYP))	V_{max} (pmol/(min·pmol of CYP))	apparent K_m (μM)	V_{max}/K_m (μL/(min·pmol of CYP))
			CYP2C8			
wild-type	1.75 ± 0.11	147 ± 9	0.0119 ± 0.0012	0.57 ± 0.001	165 ± 5	0.0034 ± 0.0001
I113V−S114F−S359I−V362L−G365S−V366L	1.05 ± 0.04[b]	179 ± 21	0.0059 ± 0.0005[b]	0.49 ± 0.04	242 ± 29	0.0020 ± 0.0001[b]
I113V−S114F	0.37 ± 0.02[b]	188 ± 17[b]	0.0020 ± 0.0001[b]	1.01 ± 0.12[b]	179 ± 22	0.0057 ± 0.0001[b]
I113V	0.67 ± 0.06[b]	320 ± 17[b]	0.0021 ± 0.0002[b]	1.25 ± 0.16[b]	243 ± 14[b]	0.0051 ± 0.0005[b]
S114F	1.13 ± 0.11[b]	206 ± 18[b]	0.0055 ± 0.0004[b]	0.92 ± 0.07[b]	297 ± 17[b]	0.0031 ± 0.0003
S359I−V362L−G365S−V366L	2.37 ± 0.17[b]	195 ± 17[b]	0.0121 ± 0.0003	0.45 ± 0.03[b]	474 ± 19[b]	0.0009 ± 0.00004[b]
S359I	1.33 ± 0.04[b]	169 ± 6	0.0079 ± 0.0002[b]	0.96 ± 0.04[b]	233 ± 6[b]	0.0041 ± 0.0002[b]
V362L	2.75 ± 0.09[b]	284 ± 6[b]	0.0097 ± 0.0004	1.70 ± 0.16[b]	1597 ± 191[b]	0.0011 ± 0.0003[b]
G365S	1.48 ± 0.15	235 ± 12[b]	0.0063 ± 0.0006[b]	0.57 ± 0.02	543 ± 46[b]	0.0011 ± 0.00003[b]
V366L	2.02 ± 0.03	215 ± 5[b]	0.0094 ± 0.0003	1.80 ± 0.03[b]	341 ± 10[b]	0.0053 ± 0.0001[b]
			CYP2C9			
wild-type	7.63 ± 1.42	12 ± 1	0.6398 ± 0.0809	0.84 ± 0.14	15 ± 2	0.0555 ± 0.0084

[a] Apparent K_m and V_{max} values are given as mean ± SD of four experiments for wild-type CYP2C8 and CYP2C8 mutants and three experiments for wild-type CYP2C9. [b] $P < 0.05$ compared to wild-type CYP2C8.

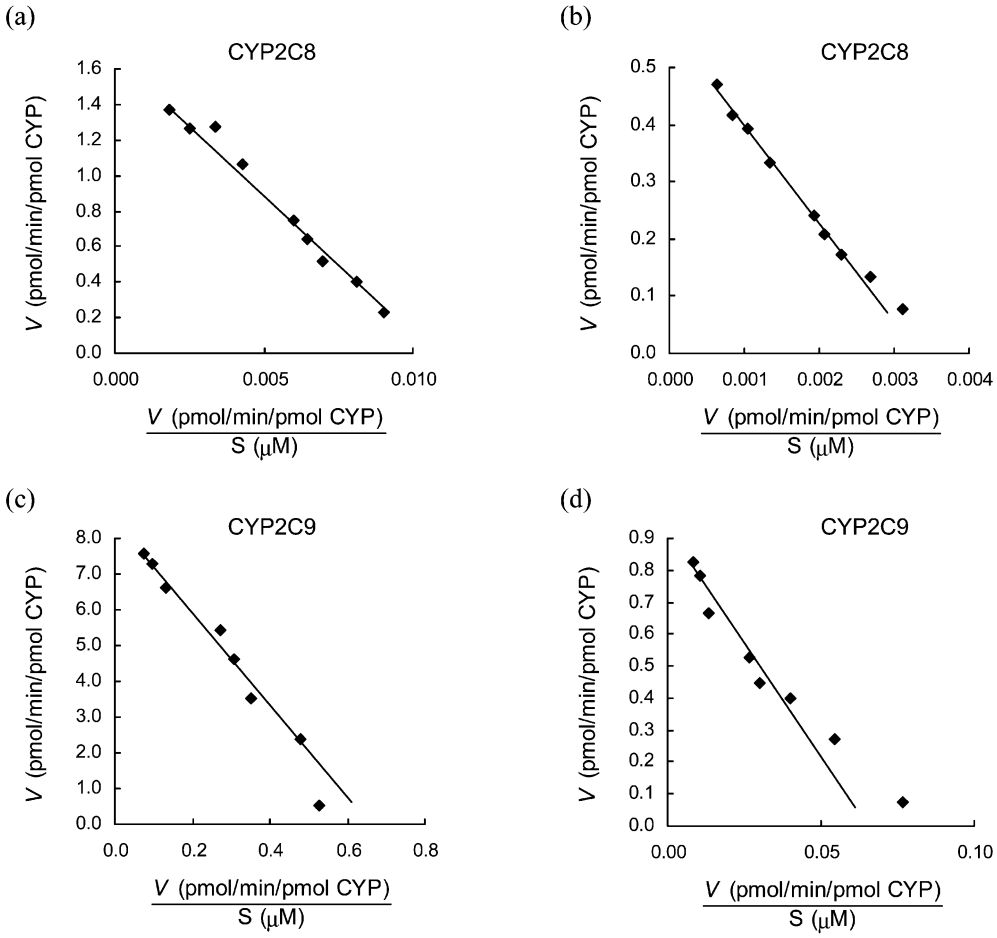

FIGURE 3: Representative Eadie−Hofstee plots for torsemide hydroxylation by wild-type CYP2C8 and CYP2C9: (a) torsemide methyl hydroxylation by CYP2C8; (b) torsemide ring hydroxylation by CYP2C8; (c) torsemide methyl hydroxylation by CYP2C9; (d) torsemide ring hydroxylation by CYP2C9. Points are experimentally determined values, while the solid lines are the computer-generated curves of best fit.

DISCUSSION

Despite increasing evidence that CYP2C8 plays an important role in the metabolism of drugs and endogenous compounds, CYP2C8 structure−function relationships are poorly understood. The ability to generate CYP2C8 site-directed mutants in heterologous expression systems based on predictions from CYP2C active site models allows a

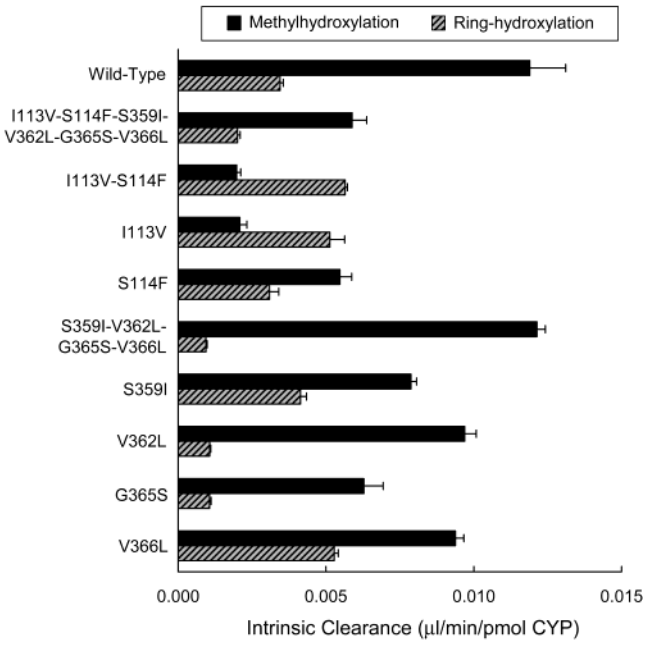

FIGURE 4: Intrinsic clearances (V_{max}/K_m) for torsemide methyl and ring hydroxylation by wild-type CYP2C8 and CYP2C8 mutants.

systematic approach to identification of the contribution of individual active site residues to substrate selectivity and regioselectivity. In this study, we have taken advantage of the sequence similarity between CYP2C8 and CYP2C9 and their different catalytic profiles to investigate the residues determining CYP2C8-like and CYP2C9-like activities. Residues 113, 114, 362, 365, and 366 of CYP2C8 were mutated on the basis of CYP2C homology models. The very recently solved CYP2C8 X-ray crystal structure (Protein Data Bank, reference 1PQ2) confirms the location of these residues in the active site. Residue 359 was additionally mutated given its known effects on CYP2C9 activity. While certain mutations in SRS1 and SRS5 abolished or greatly reduced paclitaxel 6α-hydroxylation, more subtle changes were observed for torsemide hydroxylation regioselectivity and kinetics.

Paclitaxel 6α-hydroxylation, a pathway specific for CYP2C8, was abolished by the I113V−S114F−S359I−V362L−G365S−V366L, I113V−S114F, and S359I−V362L−G365S−V366L combined mutations indicating both SRS1 and SRS5 residues were critical for paclitaxel binding, turnover, or both. Within SRS1, the single mutation S114F resulted in loss of activity. There was no significant effect of the I113V substitution on intrinsic clearance, although both K_m and V_{max} were decreased (by approximately 45%). All mutations in SRS5, except S359I, markedly affected paclitaxel 6α-hydroxylation. Activity was abolished by the V366L substitution, while the V362L and G365S mutations reduced intrinsic clearance by 94% and 88%, respectively.

Torsemide is preferentially metabolized by CYP2C9 with intrinsic clearances for methyl and ring hydroxylation being 54- and 16-fold greater for CYP2C9 compared to CYP2C8. On this basis, it was anticipated that substitution of the amino acids present in CYP2C8 for those in CYP2C9 would produce CYP2C8 mutants with higher torsemide hydroxylase activity. Indeed, there is evidence demonstrating that the functions of mammalian CYPs can be interconverted by multiple reciprocal substitutions of SRS residues (for example, ref *40*). Contrary to expectations, intrinsic clearances were either unchanged or decreased by the mutations in SRS1 and SRS5, although hydroxylation regioselectivity was often altered. With one exception (S359I), all of the individual mutations significantly increased the K_m for each pathway. The individual mutations generally either increased or caused no change in V_{max}. The notable exception in this regard was the reduced V_{max} values for torsemide methyl hydroxylation associated with the SRS1 mutations. In particular, the opposing effects of the I113V substitution on methyl and ring hydroxylation resulted in reversal of regioselectivity to favor the latter pathway (Figure 4), suggesting that this residue may be of importance for orientating smaller substrates within the active site. Only the G365S mutation significantly reduced the intrinsic clearances of both hydroxylation pathways.

S114 of CYP2C8 represents a major difference compared to other CYP2C enzymes, which have a phenylalanine at this position. In this study, the S114F substitution abolished paclitaxel 6α-hydroxylation but resulted in less than 2-fold changes in the respective K_m and V_{max} values for torsemide methyl and ring hydroxylations. It would therefore appear that hydrogen bonding with serine is important for interaction with the prototypic CYP2C8 substrate paclitaxel since the latter observation suggests that the S114F mutation does not result in major conformational changes within the CYP2C8 active site. It should be noted that the recently published X-ray crystal structure of CYP2C9 orientates the aromatic ring of F114 into the active site and places this residue in van der Waals contact with the bound substrate *S*-warfarin (*8*). Consistent with a direct binding interaction (due to $\pi-\pi$ stacking) involving this residue, site-directed mutagenesis of F114 (F114L and F114I) of CYP2C9 dramatically reduced or abolished the hydroxylation of the aromatic compounds diclofenac, tienilic acid, and *S*-warfarin but reduced lauric acid 11-hydroxylation only 2-fold (*22*, *25*). The V113L substitution in CYP2C9 has also been reported to abolish *S*-warfarin 7-hydroxylation while minimally affecting lauric acid 11-hydroxylation (*25*). V113 is also located in the hydrophobic pocket that forms the CYP2C9 active site and hydrogen bonds to R97 (*8*). The I113V mutation introduced here into CYP2C8 represents a highly conserved substitution (both β-branched hydrophobic residues). The variable influence of the I113V mutation on paclitaxel 6α-hydroxylation (no change) and torsemide hydroxylation (altered regioselectivity) would seem consistent with more subtle steric effects.

The sequences of CYP2C8 and CYP2C9 differ at four residues in SRS5: S359I, V362L, G365S, and V366L. The CYP2C9 crystal structure locates residues 362 and 364−367 in a hydrophobic active site "pocket" (*8*). Similarly, a CYP2C8 homology model constructed using CYP2C5 as the template (and the recently solved crystal structure for CYP2C8) indicates a potential role for residues 361, 362, 365, and 366 in substrate binding (*6*). Here, the combined S359I−V362L−G365S−V366L mutation abolished paclitaxel 6α-hydroxylation by CYP2C8. There was little effect arising from the S359I mutation, but each of the V362L, G365S, and V366L substitutions abolished or dramatically reduced paclitaxel 6α-hydroxylation indicating a critical role of the SRS5 residues in this pathway. All of the mutations at residues 362, 365, and 366 increased the K_m's for

torsemide methyl and ring hydroxylation. However, only G365S significantly reduced torsemide methyl-hydroxylation intrinsic clearance. Due largely to the effects of substitutions at positions 362 and 365, the intrinsic clearance for torsemide ring hydroxylation by the combined S359I−V362L−G365S−V366L mutation was decreased by 74% relative to wild-type CYP2C8. Consistent with an important role for residue 365 in CYP2C activity, the reverse substitution (i.e., S365G) in CYP2C9 has been shown to abolish diclofenac 4′-hydroxylation and reduce the intrinsic clearance for tienilic acid 5-hydroxylation by 75% (*25*).

Although residue 359 is not located in the CYP2C9 active site, or indeed the CYP2C8 active site (*6*, *8*), mutations at this position are known to influence CYP2C activity. The CYP2C9 poor-metabolizer phenotype arises from polymorphism at position 359 (viz., I359L) (*9*). Intrinsic clearances associated with the L359 variant are approximately 80% lower compared to wild-type (I359) CYP2C9 (*20*, *31*, *32*), and substitution with numerous other amino acids (including serine) has also been observed to reduce activity (S. L. Boye, D. J. Elliot, D. J. Birkett, and J. O. Miners, unpublished data). However, mutation of S359 to isoleucine (present in CYP2C9) minimally affected CYP2C8 activity toward paclitaxel and torsemide.

Paclitaxel is a large molecule (Figure 1; molecular weight 854) compared to most CYP substrates. Data presented here indicate that S114 (but not I113), V362, G365, and V366 are essential for 6α-hydroxylation, the sole metabolic pathway catalyzed by CYP2C8. Torsemide is a smaller molecule (Figure 1; molecular weight 348). CYP2C8 converts torsemide to methyl- and ring-hydroxylated metabolites, indicative of two productive binding orientations. Although mutations at residues 113, 114, 362, 365, and 366 influenced the regioselectivity of torsemide hydroxylation, none abolished metabolism. Since torsemide is preferentially metabolized by CYP2C9, the S114F and G365S substitutions in CYP2C8 might have been expected to enhance torsemide binding, turnover, or both given the roles of F114 and S365 in the CYP2C9-catalyzed metabolism of aromatic substrates (*22*, *25*). These observations suggest different active site architectures and different binding orientations of torsemide in the CYP2C8 and CYP2C9 active sites. Thus, reciprocal substitutions within the active sites are unlikely to result in interchangeability of function, although as demonstrated here for torsemide, changes in hydroxylation regioselectivity may occur. The X-ray crystal structures of CYP2C proteins indicate that these enzymes have relatively large active sites with flexible regions that adapt to substrate binding. This permits multiple binding orientations within CYP2C active sites, at least for small to moderately sized substrates (*8*, *41*). Consistent with this hypothesis, the results of the present study demonstrate that CYP2C8 active site residues differentially contribute to the binding, turnover, or both of paclitaxel and torsemide and indicate that binding orientations and the effects of amino acid substitutions within the CYP2C8 active site cannot be inferred from studies with a single substrate.

REFERENCES

1. Rendic, S. (2002) Summary of information on human CYP enzymes: Human P450 metabolism data, *Drug Metab. Rev. 34*, 83−448.
2. Lewis, D. F. V. (2003) Human cytochromes P450 associated with the phase 1 metabolism of drugs and other xenobiotics: A compilation of substrates and inhibitors of CYP1, CYP2 and CYP3 families, *Curr. Med. Chem. 10*, 1955−1972.
3. Domanski, T. L., and Halpert, J. R. (2001) Analysis of mammalian cytochrome P450 structure and function by site-directed mutagenesis, *Curr. Drug Metab. 2*, 117−137.
4. Gotoh, O. (1992) Substrate recognition sites in cytochrome P450 family 2 (CYP2) proteins inferred from comparative analyses of amino acid and coding nucleotide sequences, *J. Biol. Chem. 267*, 83−90.
5. Williams, P. A., Cosme, J., Sridhar, V., Johnson, E. F., and McRee, D. E. (2000) Mammalian microsomal cytochrome P450 monooxygenase: Structural adaptations for membrane binding and functional diversity, *Mol. Cell 5*, 121−131.
6. Ridderstrom, M., Zamora, I., Fjellstrom, O., and Andersson, T. B. (2001) Analysis of selective regions in the active sites of human cytochrome P450, 2C8, 2C9, 2C18, and 2C19 homology models using GRID/CPCA, *J. Med. Chem. 44*, 4072−4081.
7. de Groot, M. J., Alex, A. A., and Jones, B. C. (2002) Development of a combined protein and pharmacophore model for cytochrome P450 2C9, *J. Med. Chem. 45*, 1983−1993.
8. Williams, P. A., Cosme, J., Ward, A., Angove, H. C., Vinkovic, D. M., and Jhoti, H. (2003) Crystal structure of human cytochrome P450 2C9 with bound warfarin, *Nature* (13 July), 1−4.
9. Miners, J. O., and Birkett, D. J. (1998) Cytochrome P4502C9: An enzyme of major importance in drug metabolism, *Br. J. Clin. Pharmacol. 45*, 525−538.
10. Li, X.-Q., Bjorkman, A., Andersson, T. B., Ridderstrom, M., and Masimirembwa, C. M. (2002) Amodiaquine clearance and its metabolism to N-desethylamodiaquine is mediated by CYP2C8: A new high affinity and turnover enzyme-specific probe substrate, *J. Pharmacol. Exp. Ther. 300*, 399−407.
11. Muck, W. (1998) Rational assessment of the interaction profile of cerivastatin supports its low propensity for drug interactions, *Drugs 56* (Suppl 1), 15−23.
12. Projean, D., Baune, B., Farinotti, R., Flinois, J. P., Beaune, P., Taburet, A. M., and Ducharme, J. (2003) In vitro metabolism of chloroquine: identification of CYP2C8, CYP3A4, and CYP2D6 as the main isoforms catalyzing *N*-desethylchloroquine formation, *Drug Metab. Dispos. 31*, 748−754.
13. Rahman, A., Korzekwa, K. R., Grogan, J., Gonzalez, F. J., and Harris, J. W. (1994) Selective biotransformation of taxol to 6α-hydroxytaxol by human cytochrome P450 2C8, *Cancer Res. 54*, 5543−5546.
14. Bidstrup, T. B., Bjornsdottir, I., Sidelmann, U. G., Thomsen, M. S., and Hansen, K. T. (2003) CYP2C8 and CYP3A4 are the principal enzymes involved in the human in vitro biotransformation of the insulin secretagogue repaglinide, *Br. J. Clin. Pharmacol. 56*, 305−314.
15. Baldwin, S. J., Clarke, S. E., and Chenery, R. J. (1999) Characterization of the cytochrome P450 enzymes involved in the in vitro metabolism of rosiglitazone, *Br. J. Clin. Pharmacol. 48*, 424−432.
16. Tracy, T. S., Korzekwa, K. R., Gonzalez, F. J., and Wainer, I. W. (1999) Cytochrome P450 isoforms involved in metabolism of the enantiomers of verapamil and norverapamil, *Br. J. Clin. Pharmacol. 47*, 545−552.
17. Becquemont, L., Mouajjah, S., Escaffre, O., Beaune, P., Funck-Brentano, C., and Jaillon, P. (1999) Cytochrome P-450 3A4 and 2C8 are involved in zopiclone metabolism, *Drug Metab. Dispos. 27*, 1068−1073.
18. Rifkind, A. B., Lee, C., Chang, T. K., and Waxman, D. J. (1995) Arachidonic acid metabolism by human cytochrome P450s 2C8, 2C9, 2E1, and 1A2: regioselective oxygenation and evidence for a role for CYP2C enzymes in arachidonic acid epoxygenation in human liver microsomes, *Arch. Biochem. Biophys. 320*, 380−389.
19. Nadin, L., and Murray, M. (1999) Participation of CYP2C8 in retinoic acid 4-hydroxylation in human hepatic microsomes, *Biochem. Pharmacol. 58*, 1201−1208.
20. Veronese, M. E., Doecke, C. J., Mackenzie, P. I., McManus, M. E., Miners, J. O., Rees, D. L. P., Gasser, R., Meyer, U. A., and Birkett., D. J. (1993) Site-directed mutation studies of human liver cytochrome P-450 isoenzymes in the CYP2C subfamily, *Biochem. J. 289*, 533−538.
21. Klose, T. S., Ibeanu, G. C., Ghanayem, B. I., Pedersen, L. G., Li, L., Hall, S. D., and Goldstein, J. A. (1998) Identification of residues 286 and 289 as critical for conferring substrate specificity

of human CYP2C9 for diclofenac and ibuprofen, *Arch. Biochem. Biophys. 357*, 240−248.
22. Haining, R. L., Jones, J. P., Henne, K. R., Fisher, M. B., Koop, D. R., Trager, W. F., and Rettie, A. E. (1999) Enzymatic determinants of the substrate specificity of CYP2C9: Role of B′-C loop residues in providing the π-stacking anchor site for warfarin binding, *Biochemistry 38*, 3285−3292.
23. Tsao, C.-C., Wester, M. R., Ghanayem, G. G., Coulter, S. J., Chanas, B., Johnson, E. F., and Goldstein, J. A. (2001) Identification of human CYP2C19 residues that confer S-mephenytoin 4′-hydroxylase activity to CYP2C9, *Biochemistry 40*, 1937−1944.
24. Tracy, T. S., Hutzler, J. W., Haining, R. L., Rettie, A. E., Hummel, M. A., and Dickman, L. J. (2002) Polymorphic variants (CYP2C9*3 and CYP2C9*5) and the F114L active site mutation of CYP2C9: Effect of atypical kinetic metabolism profiles, *Drug Metab. Dispos. 30*, 385−390.
25. Melet, A., Assrir, N., Pascale, J., Lopez-Garcia, M. P., Marques-Soares, C., Jaouen, M., Dansette, P. M., Sari, M.-A., and Mansuy, D. (2003) Substrate selectivity of human cytochrome P450 2C9: Importance of residues 476, 365, and 114 in recognition of diclofenac and sulfaphenazole and in mechanism-based inactivation by tienilic acid, *Arch. Biochem. Biophys. 409*, 80−91.
26. Flanagan, J. U., McLaughlin, L. A., Paine, M. J. I., Sutcliffe, M. J., Roberts, G. C. K., and Wolf, C. R. (2003) Role of conserved Asp^{293} of cytochrome P450 2C9 in substrate recognition and catalytic activity, *Biochem. J. 370*, 921−926.
27. Afzelius, L., Zamora, I., Ridderstrom, M., Andersson, T. B., Karlen, A., and Masimirembwa, C. M. (2001) Competitive CYP2C9 inhibitors: Enzyme inhibition studies, protein homology modeling, and three-dimensional quantitative structure−activity relationship analysis, *Mol. Pharmacol. 59*, 909−919.
28. Lewis, D. F. V. (2002) Homology modelling of human CYP2 family enzymes based on the CYP2C5 crystal structure, *Xenobiotica 32*, 305−323.
29. Miners, J. O., Coulter, S., Birkett, D. J., and Goldstein, J. A. (2000) Torsemide metabolism by CYP2C9 variants and other CYP2C subfamily enzymes, *Pharmacogenetics 10*, 267−270.
30. Ong, C.-E., Coulter, S., Birkett, D. J., Bhasker, C. R., and Miners, J. O. (2000) The xenobiotic inhibitor profile of CYP2C8, *Br. J. Clin. Pharmacol. 50*, 573−580.
31. Sullivan-Klose, T. H., Ghanayem, B. I., Bell, D. A., Zhang, Z.-Y., Kaminsky, L. S., Shenfield, G. M., Miners, J. O., Birkett., D. J., and Goldstein, J. A. (1996) The role for the CYP2C9-Leu359 allelic variant in the tolbutamide polymorphism, *Pharmacogenetics 6*, 341−349.
32. Bhasker, C. R., Miners, J. O., Coulter, S., and Birkett, D. J. (1997) Allelic and functional variability of cytochrome P4502C9, *Pharmacogenetics 7*, 51−58.
33. Boye, S. L., Kerdpin, O., Elliott, D. J., Miners, J. O., Kelly, L., McKinnon, R. A., Bhasker, C. R., Yoovathaworn, Y., and Birkett, D. J. (2004) Optimizing bacterial expression of catalytically active human cytochromes P450: Comparison of CYP2C8 and CYP2C9, *Xenobiotica 34*, 49−60.
34. Gillam, E. M., Baba, T., Kim, B. R., Ohmori, S., and Guengerich, F. P. (1993) Expression of modified human cytochrome P450 3A4 in *Escherichia coli* and purification and reconstitution of the enzyme. *Arch. Biochem. Biophys. 305*, 123−131.
35. Omura, T., and Sato, R. (1964) The carbon monoxide binding pigment of liver microsomes: I Evidence for its hemoprotein nature, *J. Biol. Chem. 239*, 2370−2378.
36. Lowry, O. H., Rosebrough, N. J., Farr, A. L., and Randall, R. J. (1951) Protein measurement with the Folin phenol reagent, *J. Biol. Chem. 193*, 265−275.
37. Vermilion, J. L., and Coon, M. J. (1978) Purified liver microsomal NADPH-cytochrome P450 reductase: Spectral characterization of oxidation−reduction states, *J. Biol. Chem. 253*, 2694−2704.
38. Harris, J. W., Rahman, A., Kim, B. R., Guengerich, F. P., and Collins, J. M. (1994) Metabolism of taxol by human hepatic microsomes and liver slices: Participation of cytochrome P450 3A4 and an unknown P450 enzyme, *Cancer Res. 54*, 4026−4035.
39. Miners, J. O., Rees, D. L., Valente, L., Veronese, M. E., and Birkett, D. J. (1995) Human hepatic cytochrome P450 2C9 catalyzes the rate-limiting pathway of torsemide metabolism, *J. Pharmacol. Exp. Ther. 272*, 1076−1081.
40. Kumar, S., Scott, E. E., Liu, H. L., and Halpert, J. R. (2003) A rational approach to re-engineer cytochrome P450 2B1 regioselectivity based on the crystal structure of cytochrome P450 2C5, *J. Biol. Chem. 278*, 17178−17184.
41. Wester, M. R., Johnson, E. F., Marques-Soares, C., Dansette, P. M., Mansuy, D., and Stout, C. D. (2003) Structure of a substrate complex of mammalian cytochrome P450 2C5 at 2.3 Å resolution: Evidence for multiple substrate binding modes. *Biochemistry 42*, 6370−6379.

BI0496844